



GAMMA-1 Emission of Prompt Fission Gamma-Rays in Fission and Related Topics

Indication of anisotropic TKE and mass emission in $^{234}\text{U}(\text{n},\text{f})$ A. Al-Adili ^{a,b,*}, F.-J. Hambsch ^b, S. Pomp ^a, S. Oberstedt ^b^a Division of Applied Nuclear Physics, Uppsala University, S-751 20 Uppsala, Sweden^b European Commission, DG Joint Research Centre (IRMM), B-2440 Geel, Belgium

Abstract

The neutron-induced fission of ^{234}U has been studied for neutron energies ranging from 200 keV to 5 MeV. Special focus was put around the prominent vibrational resonance in the sub-barrier region around 800 keV incident neutron energy. The aim was to investigate the fission fragment (FF) characteristics and search for fluctuations in energy and mass distributions. The strong angular anisotropy in the case of $^{234}\text{U}(\text{n},\text{f})$ was verified and correlations with changes in energy and mass distributions were found. The TKE around the resonance increases contrary to earlier literature data. Furthermore, the TKE and mass distribution were found to be dependent on emission angle. At the resonance, the TKE was smallest near the 0° emission of the FF. This effect was consistent and coherent with a change in the mass distribution around the resonance. The mass distribution was observed to be less asymmetric near 0° emission. From a fitting analysis based on the Multi-Modal Random Neck-Rupture (MMRNR) model, we found the yield of the standard-1 mode increasing around the resonance. Because the TKE is increasing at larger angles and the mass distribution becomes more symmetric also at larger angles, we conclude that this behavior is due to an increase of the standard-1 mode at these larger angles. Based on the formalism of MMRNR, such difference in angular distribution may be an indication of a different outer barrier height for the standard-1 and standard-2 modes.

© 2012 Published by Elsevier B.V. Selection and/or peer-review under responsibility of Institute for Reference Materials and Measurements. Open access under [CC BY-NC-ND license](https://creativecommons.org/licenses/by-nc-nd/4.0/).

Keywords: ^{234}U , anisotropy, TKE and mass yield distributions.

1. Introduction

The nuclear libraries lack data for the neutron-induced fission of ^{234}U , particularly concerning the fission fragment (FF) energy distribution and mass yield. The only experimental work known to the authors investigating the FF properties is Ref. [1]. However, the angular anisotropy of $^{234}\text{U}(\text{n},\text{f})$ has been investigated extensively [2,3,4]. The reason is that $^{234}\text{U}(\text{n},\text{f})$ exhibits extraordinary fluctuations from largely negative to largely positive emission-angle anisotropies around the prominent vibrational resonance at 800 keV incident neutron energy. Due to this very strong anisotropic behavior, it would be

interesting to investigate the FF characteristics. In the present work these FF characteristics are measured, by means of a Twin Frisch-Grid Ionization Chamber (TFGIC). The neutrons were produced at the 7MV Van de Graaff accelerator at the Institute for Reference Materials and Measurements (IRMM) in Geel, Belgium.

2. Experiment

The experimental setup was described in detail in Ref. [5]. The TFGIC, which consists of two anode plates, two Frisch grids and one common cathode, detects the FF simultaneously on each chamber side. The FF ionizes the counting gas (P-10) leaving free electron-ion pairs. These induce an electric signal while drifting towards the anode plates. The total charge induced on the anode plates is proportional to the fragment energy, while the induced charge on the Frisch grid reveals information on the fragment emission angle. The signals were read out by means of a parallel analogue and digital data-acquisition system. A comparison of both systems was carried out to search for possible improvements with the modern digital techniques and was discussed in Refs. [5,6]. The collinear fragment emission is used along with the conservation of energy and mass to calculate iteratively the FF pre-neutron emission mass and energy. As an absolute energy calibration, $^{235}\text{U}(n,f)$ at thermal energy was used since the literature data are well known.

3. Data analysis

3.1. Signal treatment

The raw digital data needed to be treated for various effects such as corrections of the signal offset, ballistic deficit and alpha pile-up. In the case of ^{234}U about 150,000 α particles are emitted per second, compared to a maximum event rate from the neutron induced fission of 10 FF/sec. The window of charge collection of the acquisition system was set to 10 μsec , so practically each fragment had a contribution of at least one α particle. By application of digital-signal processing, it was possible to correct for over 90% of these coincidences. Depending on the rise time for each fission event, which was determined event-by-event, the α -particles outside a small integration window were deleted. Hence, the fission events showing pile-up could be corrected and further used in the analysis without discarding them as it was the case in analogue acquisition. This correction possibility was the main advantage found by applying the digital techniques [5]. Another important advantage concerns the fragment emission angle and was presented in Ref. [6]. To calculate the emission angle, the “summing method” is usually applied. The principle is to use the charge induced on the Frisch grid to determine the angle. But due to its bipolarity, the grid signal was always summed together with the anode signal. This operation preserves the angle-information in the grid signal, but leaves only a unipolar signal convenient to treat in conventional analogue electronics. The procedure relies on a stable and perfectly calibrated signal since two different pre-amplifier signals were summed together. By using solely the grid signal, we improved the angular resolution due to the higher stability [6]. This could only be achieved by using digital-signal processing. The signal treatment finishes after determining the height of the anode and grid signals. For the pulse height determination i.e. of the anode signal, a CR-RC⁴ filter was used to optimize the signal to noise ratio.

3.2. Fragment analysis

Once the pulse heights were determined from the raw signals, further analysis was carried out. The following corrections had to be accounted for:

1. A proper correction for the grid-inefficiency: For details see Refs. [6,7,8].
2. A correction for the pulse-height defect, based on a parameterization from Ref. [9].
3. A correction of the neutron-momentum transfer and finally the crucial energy-loss corrections.

Once all these effects have been accounted for, the FF masses can be calculated iteratively. However, since no neutrons are detected in the experiments, the neutron multiplicity ν (needed for the calculations) must be parameterized. The “saw-tooth” shape describes the mass dependency of ν , and was deduced using experimental data from neighboring uranium isotopes. The multiplicity is also TKE dependent as discussed in Ref. [9]. Finally, ν is also dependent on the incident neutron energy. This was parameterized based on a linear regression of experimental data taken from Ref. [10].

4. Results

The results presented in this work are based on measurements at 14 different incident neutron energies, namely: 0.2, 0.35, 0.5, 0.64, 0.77, 0.835, 0.9, 1.0, 1.5, 2.0, 2.5, 3.0, 4.0 and 5.0 MeV. For the lower neutron energies (<1 MeV) the reaction $\text{Li}(p,n)$ was used whereas $\text{TiT}(p,n)$ and $\text{D}(d,n)$ were used for higher energies. The latter reactions provide better beam-statistics but less precision in the neutron beam energy due to the neutron producing target thickness.

4.1. Angular anisotropy

The emission angle in the laboratory system was transformed to the center-of-mass system and averaged for both chamber sides. In the case of the reference reaction $^{235}\text{U}(n_{\text{thermal}},f)$, an isotropic emission was expected and verified. In order to minimize experimental effects, the ratio of the ^{234}U and ^{235}U cosine distributions was used. To calculate the angular anisotropy each ratio from each measurement, was fitted with a Legendre polynomial of the second even order. The fit was restricted to an angle range of $0.25 < \cos(\theta) < 0.9$ in order to minimize the contribution from a worse resolution and statistical effects. The angular anisotropy over the whole incident neutron energy range is shown in Fig. 1. The trend agrees with earlier measurements from Refs. [2,3,4], showing strong changes from favorably 90° emission around 500 keV to favorable 0° around the resonance peak of 800 keV.

4.2. TKE

The energy release for the whole range and especially around the vibrational resonance was studied in terms of TKE. The change of TKE is shown in Fig. 2 and is compared to the earlier measurement of Ref. [1]. The TKE around the resonance were found to increase in our work which contradicts with the trend found in Ref. [1]. A possible explanation to the difference is discussed later. The TKE at higher incident neutron energy from 3 MeV to 5 MeV shows a decreasing trend, similar to the one found for $^{235}\text{U}(n,f)$ (see Ref. [11]).

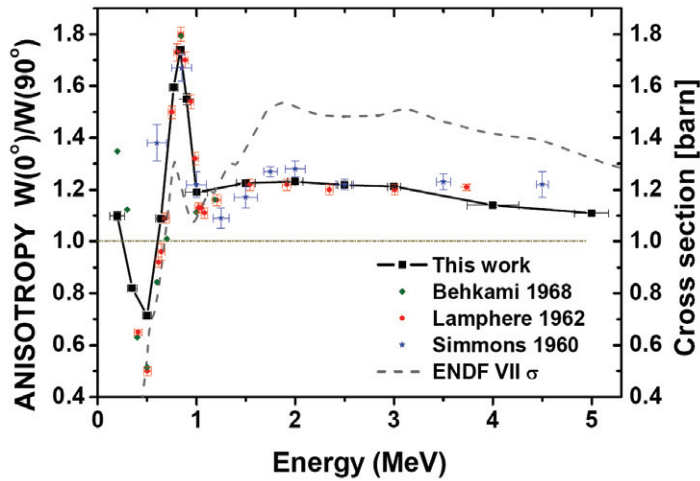


Figure 1: The angular anisotropy for $^{234}\text{U}(n,f)$. A very strong trend is observed before and at the vibrational resonance, which agrees well with literature [2,3,4]. The parameters were obtained from a Legendre polynomial fit of the second even order.

In order to further understand the energy changes, the approach of Refs. [12,13] was applied. The TKE change was expressed in terms of either direct changes in TKE or changes in mass distribution leading indirectly to TKE changes. It was found that the main changes to the TKE came from direct changes in TKE leaving a nearly constant contribution from the FF mass distribution changes. However around the resonance, the TKE change was not only a result of direct TKE changes but also from a slight change in mass distribution.

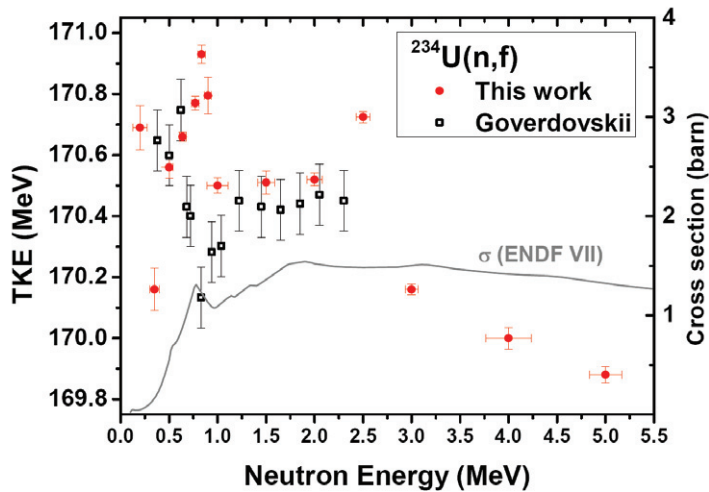


Figure 2: Changes of the TKE compared to Ref. [1]. Note the opposite trend at the resonance, around 800 keV. Only $\cos\theta > 0.5$ have been included in this work, due to angular resolution effects. In case of Ref. [1], a small solid angle was covered near the 0° emission.

4.3. Parameterization using the Multi-Modal Random Neck-Rupture (MMRNR) model

A parameterization of the mass versus TKE distributions was performed using the MMRNR model [14]. Six functions (Gaussians for the mass yield distribution and skewed Gaussians for the TKE distributions), corresponding to the different fission modes, were used in the fitting of the 2-dimensional distribution, with a total of 18 fit parameters as described in Refs. [9,13]. The standard-2 yield is usually dominant and in our case it is responsible for 80-90 % of all fission events. The fitting procedure was in general very well describing both TKE and mass distributions ($\chi^2 \sim 1$). The results from the mode analysis showed an increased yield of standard-1 at the resonance. Standard-1 is responsible for the more energetic fission events, because it is attributed to a more compact shape. Hence, one consequence of the higher Standard-1 yield is a larger TKE in the vicinity of the resonance.

5. Discussion

In the present work, the TKE as a function of incident neutron energy was found significantly different around the resonance compared to Ref. [1], as seen in Fig. 2. This opens the question of the nature of vibrational resonances. Is a lower TKE a requisite for vibrational resonances? To identify possible causes to the diverse observations, the experimental conditions will be discussed. It is proposed that the difference in TKE is due to an anisotropic FF TKE and mass emission.

Firstly, in our case, using a TFGIC, a wider solid angle has been covered. Whereas, using a surface barrier detector in the geometry as given in Ref. [1], leaves most emission angles uncovered. Secondly, in Ref. [1], two geometries were studied individually (around 0° and 90°). The presented results from Ref. [1], showed that at the resonance peak, the TKE is more than 1 MeV higher at 90° than at 0° . This angle-dependent effect was not found outside the resonance peak. However the authors choose to present the data from 0° only as being fission through the vibrational resonance. In our case, the clear trend of a higher TKE was removed when only events near 0° were considered. In fact, we observe, that the higher TKE around the resonance is mainly caused by the fragments emitted at larger angles (see Fig. 3). In the beam axis direction (i.e. 0°), the TKE seems slightly lower than outside the resonance.

A change in TKE must be studied with a possible change of the FF mass distribution. As discussed earlier, the MMRNR-mode analysis implied a larger standard-1 yield at the resonance. Moreover, from the individual TKE contributions, a change in mass distribution was found to contribute to the TKE change at the resonance. The final step is to link this mass change with the angle dependency of the TKE. A linear fit to the mean mass as a function of cosine, for all measurements, resulted in a greater mass difference at the resonance peak. Clearly this indicated that the largest change of the mass distribution, between 0° and 90° was found at the resonance. The mass distribution becomes more symmetric for emission angles of 90° . Hence naturally, the TKE must increase for these emission angles. Since the yield of the standard-1 mode is growing, we can attribute this mode change to parts of the angle range. Thus, the standard-1 mode increases around the resonance for higher emission angles. It is of interest that such angle dependencies correlate to the vibrational resonance, especially since the angular distribution changes so drastically.

An angle dependent FF mass and TKE distribution may not have been widely discussed and realized, in earlier works. The classical fission model fails to explain such behavior as discussed in Ref. [15]. Hence, this idea has been rejected in the past, despite a few experimental studies which supports a mass anisotropy e.g. the case of $^{235}\text{U}(n,f)$ [16] and ^{232}Th , $^{236,238}\text{U}$ [17]. However within the MMRNR model such mass emission anisotropies are embedded in the model as described in Ref. [18]. The MMRNR model predicts different outer fission barriers for the different modes (see e.g. the calculations performed

for $^{238}\text{U}(n,f)$ [19]). Assuming for each fission mode a different pre-scission shape with respective different fission fragment properties, then the superposition could lead to differences in the observables in experiment as has been found in the present work. In fact different angular distributions in the different fission modes may be attributed to a different outer fission barrier height. Hence this result could be the first proof of individual outer fission barriers.

In conclusion, our results have an important consequence to this kind of FF experiment and analysis. It is crucial to choose the right method of energy-loss correction, in order not to remove these physical effects. By applying the wrong correction method, one may remove the angular dependency in the energy distribution, since it is corrected as a part of the energy losses. The proper energy-loss correction is to keep the correction curve constant when treating measurements with different incident neutron energies. In this way, the correction is only dependent on the emission angle. In contrary, by applying an individual energy loss curve to each measurement, the correction is also dependent on the initial fragment kinetic energy.

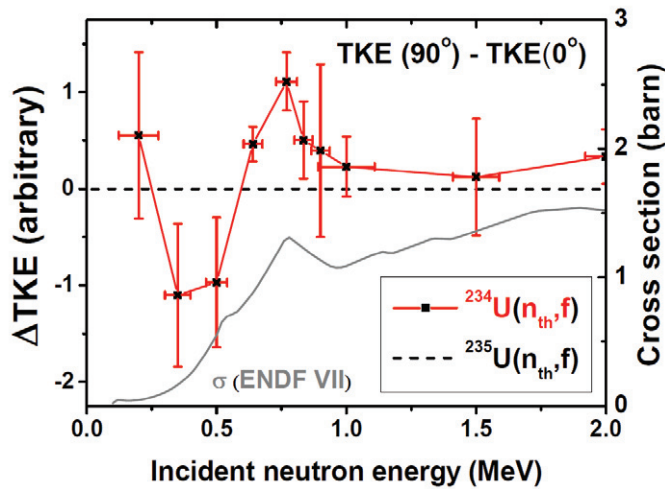


Figure 3: The TKE angular dependency as a function of incident neutron energy: On the y-axis, the relative difference between the TKE at 90° and 0° is shown in arbitrary unit. At the resonance the TKE at angles of 90° is largest compared to 0° emission. Whereas at $E_n = 350\text{ keV}$ - 500 keV the difference in TKE is at largest at 0° compared to the 90° emission angles. At $\Delta\text{TKE}=0$, $^{235}\text{U}(n_{th},f)$ is found where TKE is supposed to be isotropic [16].

6. Conclusions

In this work we have investigate the $^{234}\text{U}(n,f)$ reaction from 0.2 MeV to 5 MeV, using a TFGIC. The study was based on digital-data acquisition systems and compared to conventional analogue techniques. The digital techniques improve the drift stability and opens up novel possibilities e.g. alpha pile-up correction. Also, we enhanced the angular resolution by improving the emission angle extraction. The results concerning the angular anisotropy were in good agreement with several earlier literature data. A strong forward directed emission was found at the prominent vibrational resonance peak around 800 keV incident neutron energy. The correlations with other observables such as the FF TKE and mass distributions were studied as well. The TKE as a function of the incident neutron energy was larger in the vicinity of the vibrational resonance. This is contrary to the earlier reported measurement where the TKE

decreased at the resonance. A possible explanation of this opposite trend is the solid angle coverage. In this work we have a nearly 4π coverage, compared to the limited angular range with the set-up of Ref. [1]. By studying the angle dependence on the energy distributions a correlation was found with the resonance. The fragments emitted near 0° relative to the neutron beam, have lower TKE compared to fragments emitted at larger angles. The largest change in fragment energy between 0° and 90° emission was found around the resonance. By selecting only emission angles near 0° , the TKE was not larger at the resonance. Finally the FF mass distributions also showed an angular dependency, which was highest at the vibrational resonance. The mass distribution at the resonance becomes more symmetric for higher emission angles. As consequence of the more symmetric distributions a higher TKE is expected, which is consistent with the TKE findings at larger emission angles. After a parameterization of the results in terms of the MMRNR model it was concluded that the yield of the standard 1 mode increased at the resonance for larger emission angles. These findings support the idea of an angle dependent yield variation of the different fission modes. The angular dependent TKE and mass emission may be indicating an important property of the fission barrier. Namely, that the outer fission barrier may be of a different height for standard-1 and standard-2 modes. The MMRNR model would support this statement as the angle dependency is embedded in the formalism [18].

References

- [1] A. Goverdovskii, B.D. Kuzminov, V.F. Mitrofanov and I. Sergachev, *Sov. Jour. Nucl. Phys.* 44 (1986) 287.
- [2] J. Simmons and R. L. Henkel, *Phys. Rev.* 120 (1960) 198.
- [3] R. Lamphere, *Nuclear Physics* 38 (1962) 561.
- [4] A. Behkami, J. Roberts, W. Loveland, and J. Huizenga, *Phys. Rev.* 171 (1968) 1267.
- [5] A. Al-Adili, F.-J. Hambsch, S. Oberstedt, S. Pomp and Sh. Zeynalov, *Nucl. Instr. Methods A* 624 (2010) 684.
- [6] A. Al-Adili, F.-J. Hambsch, R. Bencardino, S. Pomp, S. Oberstedt and Sh. Zeynalov, *Nucl. Instr. Methods A* 671 (2012) 103.
- [7] A. Göök, F.-J. Hambsch, A. Oberstedt and S. Oberstedt, *Nucl. Instr. Methods A* 664 (2012) 289.
- [8] A. Al-Adili, F.-J. Hambsch, R. Bencardino, S. Pomp and S. Oberstedt, *Nucl. Instr. and Meth. A* 673 (2012) 116.
- [9] E. Birgeresson, A. Oberstedt, S. Oberstedt and F.-J. Hambsch, *Nuclear Physics A* 817 (2009) 1.
- [10] D.S. Mather, P. Fieldhouse and A. Moat, *Nuclear Physics.* 66 (1965) 149.
- [11] Ch. Straede, C. Budtz-Jørgensen and H.-H. Knitter, *Nuclear Physics A* 462 (1987) 85.
- [12] S. Pommé, E. Jacobs, M. Piessens, D. De Frenne, K. Govaert and M.-L. Yoneama, *Nuclear Physics A* 572 (1994) 237.
- [13] F. Vives, F.-J. Hambsch, H. Bax and S. Oberstedt, *Nuclear Physics A* 662 (2000) 63.
- [14] U. Brosa, S. Grossmann, and A. Müller, *Phys. Rep.* 197 (1990) 167.
- [15] R. Vandenbosch and J.R. Huizenga, *Nuclear Fission*, ACADEMIC PRESS (1973) 210.
- [16] S.S. Kapoor, D.M. Nadkarni, R. Ramanna, P.N. Rama Rao, *Physical Review.* B137 (1965) 511.
- [17] B.M. Gokhberg, L.D. Kozlov, S.K. Lisin, L.N. Morozov and V.A. Pchelin, *Sov. Jour. Nucl. Phys.* 47 (2), (1988) 320.
- [18] C. Wagemans, *The Fission Process*, CRC Press (1991) 494.
- [19] S. Oberstedt, F.-J. Hambsch, F. Vives, *Nuclear Physics A* 644 (1998) 289.